Journal of Materials Chemistry

www.rsc.org/materials

Volume 22 | Number 15 | 21 April 2012 | Pages 7059–7634

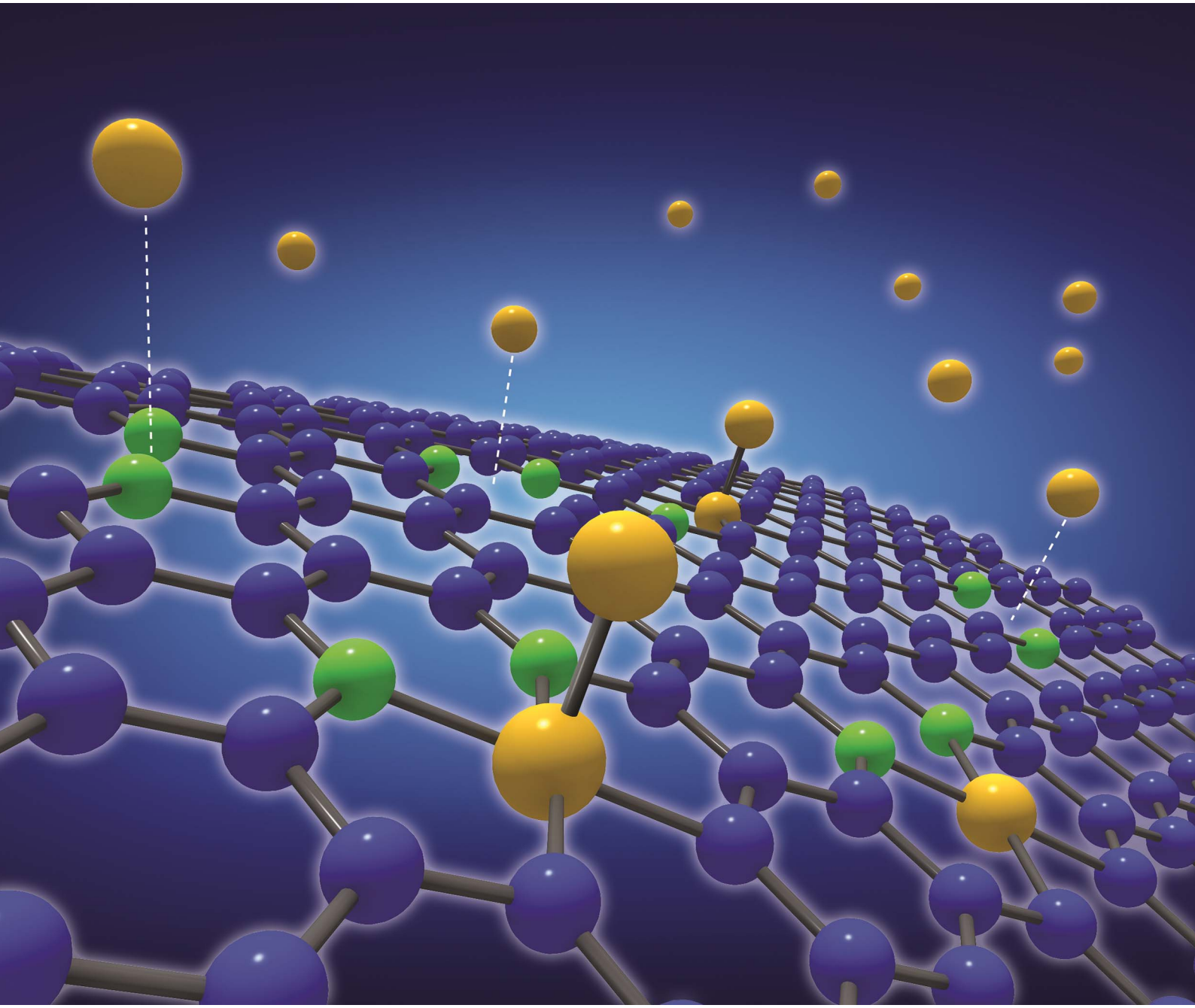

ISSN 0959-9428

RSC Publishing

PAPER

Won San Choi *et al.*

Gold nanoparticle-doped graphene nanosheets: sub-nanosized gold clusters nucleate and grow at the nitrogen-induced defects on graphene surfaces

Journal of Materials Chemistry

Dynamic Article Links

Cite this: J. Mater. Chem., 2012, 22, 7130

www.rsc.org/materials

PAPER

Gold nanoparticle-doped graphene nanosheets: sub-nanosized gold clusters nucleate and grow at the nitrogen-induced defects on graphene surfaces†

Hye Young Koo,[a] Ha-Jin Lee,[b] Yong-Young Noh,[c] Eui-Sup Lee,[d] Yong-Hyun Kim[d] and Won San Choi*[e]

Received 28th November 2011, Accepted 26th January 2012
DOI: 10.1039/c2jm16195h

We report the theory and synthesis of sub-nanosized gold clusters on reduced graphene oxide (r-GOs). The Au sub-nanoclusters were found to be nucleated and grown at defects of the r-GOs, particularly on nitrogen-induced defects from density functional theory investigation. The resulting Au/r-GOs exhibit an improvement of bulk electrical conductivities and a reduced ratio of the intensity of the D band to that of the G band (I_D/I_G), compared to the r-GOs without Au nanoclusters. The unique decrease of the I_D/I_G was demonstrated to be related to the filling of subnano-sized Au clusters on the r-GOs, presumably owing to enhancing the flat geometry of the graphene nanosheets.

Introduction

Graphene nanosheets (GNS), a single layer consisting of sp^2-bonded carbon atoms, attract considerable scientific interest because of their excellent thermal, mechanical, and electronic properties.[1] In order to realize their technological application, mass production of graphene is essential. Among various approaches, the chemical exfoliation of graphite through oxidation is one of the potential methods of achieving this goal.[2] However, compared to other production methods such as mechanical exfoliation or chemical vapor deposition (CVD), chemical exfoliation generally causes substantial damage to the graphene structure. The defects like vacancies, oxide functionalities, and substitutional nitrogen formed by harsh chemical treatments perturb the π–π network of graphene, inducing a loss of electrical conductivity of the resulting reduced graphene oxide (r-GO) structure. Thus, significant efforts have been put toward recovering a reasonable level of conductivity by methods such as molecular doping, electrochemical doping, thermal annealing, and creating composites with other materials.[3]

The functionalization of GNSs with inorganic nanoparticles (NPs) to manipulate their electrical, structural, and interfacial properties has been the subject of recent investigations.[4] For example, GNS composites with gold, platinum, palladium, and silver NPs have been investigated for novel catalytic, magnetic, and optoelectronic properties.[5] In these composite structures, GNSs act as a substrate for supporting the adhered metal NPs. With the benefit of the large specific surface area of the GNSs, the resulting composites can exhibit enhanced properties for adsorption and sensing applications. As a noteworthy example, Yoo *et al.* reported enhanced electrocatalytic activity of GNSs composited with Pt sub-nanoclusters.[6] In their work, presence of extremely small Pt clusters on the GNSs enabled a strong interaction between the GNSs and Pt atoms. The authors demonstrated that the stability of the Pt clusters is higher at the defect sites of the GNSs than at the defect-free sites.

In this report, we demonstrate that the growth of sub-nanosized Au clusters on r-GOs can reinforce the conductivity of the resulting r-GOs by defect filling. Raman studies on the resulting AuNP/r-GOs indicated a unique decrease of the I_D/I_G ratio and a concurrent increase of the conductivity upon repeated growth of the AuNPs. Here, I_D/I_G represents the ratio of the intensity of the D band to that of the G band, and this ratio is widely used for inferring defect density in graphitic materials.[7] Several reports on the AuNP/r-GOs composites and their corresponding Raman studies indicated nominal increases of the I_D/I_G ratio.[8] In this report, however, successive decrease of the I_D/I_G ratio upon repeated growth of the AuNPs were observed. This phenomenon was found to be related to the presence of sub-nanosized Au clusters on the GNSs. The extent of the change in the electrical conductivity and the I_D/I_G ratio of the AuNP/GNSs could be controlled by variation of the AuNP growth cycles. Also, the conductivity and the I_D/I_G ratio could be restored to their initial values for the pristine r-GOs when the sub-nano Au clusters that filled the defects were eliminated. These results demonstrate the direct effect of the AuNPs on the electronic structure of the AuNP/r-GO composites. The mechanism for the defect filling of

[a]*Institute of Advanced Composite Materials, Korea Institute of Science and Technology (KIST), Jeonbuk, 565902, South Korea*
[b]*Jeonju Center, Korea Basic Science Institute (KBSI), Dukjin-dong 1ga, Dukjin-gu, Jeonju, 561-756, South Korea*
[c]*Department of Chemical Engineering, Hanbat National University, San 16-1, Dukmyung dong, Yuseong-gu, Daejeon, 305719, South Korea*
[d]*Graduate School of Nanoscience and Technology (WCU), Korea Advanced Institute of Science and Technology (KAIST), Daejeon, 305701, South Korea*
[e]*Department of Applied Chemistry, Hanbat National University, San 16-1, Dukmyung dong, Yuseong-gu, Daejeon, 305719, South Korea. E-mail: choiws@hanbat.ac.kr; Fax: (+)82-42-821-1692*
† Electronic supplementary information (ESI) available: See DOI: 10.1039/c2jm16195h

r-GO was verified by density-functional theory (DFT) calculations.

Results and discussion

The Au/r-GO composites were prepared from graphite in two steps: (1) r-GOs were obtained by reducing exfoliated graphite oxide according to the method described in the literature;[9] (2) the AuNPs were synthesized on the surface of the r-GOs by incubation of the r-GOs in a chloroauric acid ($HAuCl_4$) solution and subsequent reduction with sodium borohydride ($NaBH_4$). For controlled growth of the AuNPs, the reaction was repeated between one and four times (see the ESI† for more details). No damage on the r-GOs upon successive $NaBH_4$ treatment was confirmed by Raman spectroscopy (data not shown). The Au/r-GO composites obtained from one to four reaction cycles are hereafter named 1-, 2-, 3-, and 4-Au/r-GOs, respectively. For obtaining small AuNPs with a relatively uniform size distribution, optimal concentrations of the chloroauric acid and the GNSs are surely necessary.

The effects of the growth of AuNPs on the electronic structure of the r-GOs were investigated by Raman scattering signal analysis (Fig. 1). The Raman spectra showed three normal peaks from graphenes: a D band (1325 cm^{-1}), a G band (1572 cm^{-1}), and a 2D band (2626 cm^{-1}). Due to the chemically harsh preparation method, the r-GOs prepared in this study should contain numerous carbon vacancies and defects. Correspondingly, the intensity of the D band is higher than that of the G band for the as-synthesized r-GOs (black line). Growth of the AuNPs on the r-GOs induced changes in the electronic structure of the resulting r-GOs. After growth of the AuNPs, the G band is observed at approximately 1562 cm^{-1}(blue line), which is shifted to a lower frequency compared to the pristine GNSs (1572 cm^{-1}) (inset of Fig. 1). This G-band softening represents a well-known effect for graphenes doped with an electron donor.[10] Thus, the AuNPs here can be reasonably assumed to act as weak electron donors that induce a charge transfer from the Au clusters to the r-GOs.[11]

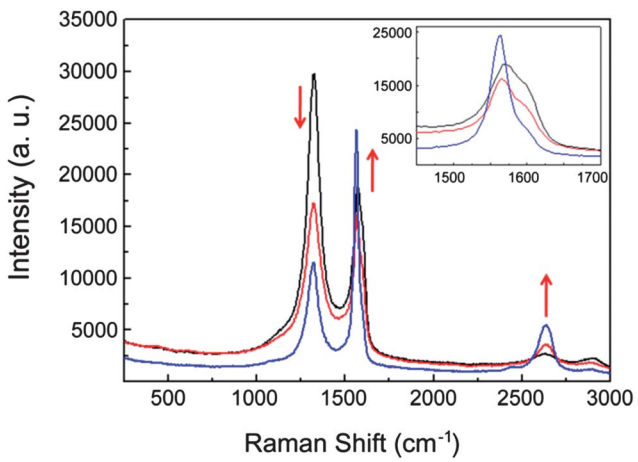

Fig. 1 Raman spectra showing the evolution of the D and G bands of the AuNP/r-GOs as a function of AuNP growth cycles (black: pristine r-GOs, red: 3-AuNP/r-GOs, blue: 4-AuNP/r-GOs, respectively). The inset is the magnified graph of the G band, showing shifts to a lower frequency upon increasing number of the growth cycles.

One distinctive feature of the Raman spectra is a decrease of the D-band intensity that accompanies simultaneous increase of the G-band intensity upon successive growth of the AuNPs. This leads to a dramatic decrease on the I_D/I_G ratio of the resulting AuNP/r-GOs (from 1.52 for the pristine GNSs to 0.45 for the 4-AuNP/r-GOs, respectively). The G-band intensity can be increased by increasing number of graphene layers. In this work, the AuNP/r-GOs are stably dispersed without aggregation or restacking. Thus, from this observation we can exclude effect of number of layers as a cause of the increase in the G-band intensity. The decrease of the D-band intensity and the consequent decrease of the I_D/I_G ratio are unusual because most of the previous works on the Raman characteristics of r-GOs composited with the AuNPs reported a nominal increase of the I_D/I_G ratio.[8] Thus, this phenomenon cannot be fully explained with only a charge-transfer mechanism.

To confirm the effect of the AuNPs on the r-GOs, we observed changes in the Raman characteristics after removal of the AuNPs by treatment with potassium cyanide (KCN) (Fig. S1†). Notably, elimination of the AuNPs from the r-GOs resulted in the recovery of the I_D/I_G ratio to a value similar to that of the pristine r-GOs. Upon treatment with KCN for 30 min, the I_D/I_G ratio increased to 1.34 (red), and this value further increased to 1.42 upon prolonged KCN treatment (blue). After complete removal of the AuNPs, the G band upshifted to 1571 cm^{-1}, which is similar to the band position of the pristine r-GOs (blue). The features of the Raman spectra of the 4-AuNP/r-GOs after elimination of the AuNPs nearly matched those of the pristine r-GOs. The r-GO was not damaged by treatment of the KCN under our conditions (data not shown). Thus, it can be concluded that the electronic structure of the r-GO can be tuned by introduction of the AuNPs and the Raman spectra reflect these changes.

Taking into consideration the successive decrease of the I_D/I_G ratio as the growth of the AuNPs proceeded, the AuNPs probably contributed to the reduction of defects in the r-GOs and the subsequent increase in their conductivity. Fig. 2 shows the changes in the conductivity and I_D/I_G ratio as a function of the reaction cycle of AuNP growth. The conductivity increased up to 9290 S m^{-1} for four repetitions of the growth cycle, which is about five times higher than that of the pristine r-GOs (black

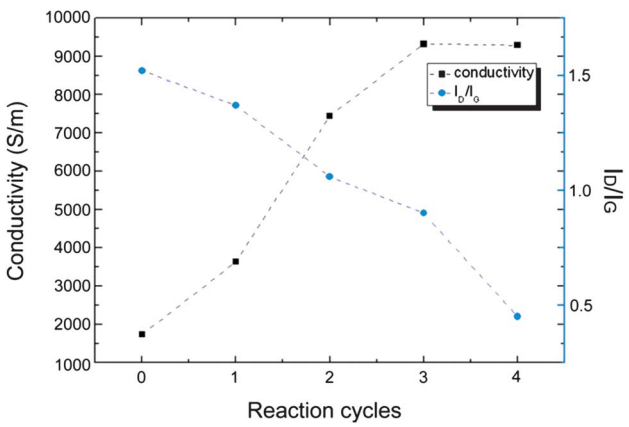

Fig. 2 Changes in the conductivities and the I_D/I_G of the AuNP/r-GOs as a function of the number of AuNP growth cycles.

squares). It is predicted that r-GOs of higher quality would show more dramatic enhancement on conductivity. The I_D/I_G ratio decreased throughout four reaction cycles (blue circles), after which the conductivity and the I_D/I_G ratio tended to saturate without further changes. The reason for this saturation is unclear and a more detailed study of this behavior is ongoing. The 4-AuNP/r-GOs treated with KCN for 30 min exhibited a reduced conductivity of approximately 3380 S m^{-1}, and this value further decreased to an initial value of approximately 1710 S m^{-1} for the pristine r-GOs upon prolonged treatment (Fig. S2†). A concurrent increase of the I_D/I_G ratio was observed as well. These results demonstrate that the growth of the AuNPs contributes to the reduction of defects in the r-GOs and the subsequent increase of conductivity. According to the literature, nucleation of the Au clusters tends to populate the defective sites of the r-GOs, such as a lattice vacancy or a reconstructed area.[12] Studies on defect filling mechanism by the Au clusters would be discussed in the simulation section.

To examine the size and distribution of the AuNPs on the r-GOs, imaging with high-angle annular dark-field scanning transmission electron microscopy (HAADF-STEM) was carried out (Fig. 3). After one reaction cycle, sub-nanosized Au clusters less than 0.5 nm in size were sparsely distributed over the surfaces of the r-GOs (Fig. 3a, 3c, and S3a). The synthesis of the AuNPs was confirmed by EDX analysis (Fig. S4†). As the growth cycle was repeated, the population of the Au subnanoclusters increased and larger Au particles appeared more frequently (Fig. 3b and 3d). The size distribution of the AuNPs broadened because nucleation and growth occurred simultaneously. As a result, the 4-AuNP/r-GOs contain AuNPs ranging in size from sub-nanometres to several sub-micrometres (Fig. S3b, S5, and S6†). When we carried out the KCN treatment for 30 min on the 4-AuNP/r-GOs, significant number of the sub-nano Au clusters was removed from the surface of the GNSs, but larger particles still remained (Fig. S6†). In this case, the changes in the I_D/I_G ratio and corresponding conductivity were not dramatic. From these results, we conclude that presence of the sub-nanosized Au clusters is crucial for the dramatic decrease of the I_D/I_G ratio and the accompanying increase in the conductivity. Indeed, numerous reports have proposed the possibility of filing defects in r-GOs by introducing metal nanoclusters on their surfaces. Yoo *et al.* reported the formation of sub-nanosized Pt clusters on the defect sites of graphenes by strong interactions between the graphenes and Pt atoms.[6] Also, Okamoto *et al.* have reported that the stability of the metal clusters on graphenes containing carbon vacancies was higher than that on defect-free graphenes.[13] Thus, it is reasonable to assume that the sub-nanosized Au clusters fill the defects, and it leads to the decrease of the I_D/I_G ratio and the corresponding increase in the conductivity of the 4-Au/r-GOs.

To elucidate the effects of larger-sized AuNPs on the conductivity of the resulting r-GOs, Au nanorods (AuNR, average diameter of 15 nm and length of 45 nm) were synthesized and adsorbed on the r-GOs. The r-GOs used in this study were functionalized with carboxylate groups, thus the cationic AuNRs could attach to the surface of the r-GOs by electrostatic interactions. Fig. 4 shows two TEM images of the resulting r-GOs with different loadings of AuNRs. The average I_D/I_G ratios are 1.53 and 1.57 for the two samples, which demonstrates a negligible effect of the amount of AuNRs on the I_D/I_G ratio (1.52) of the r-GOs. Compared to the pristine r-GOs (1720 S m^{-1}), conductivities increased to 2050 S m^{-1} and 2380 S m^{-1} for the low and high loadings of the AuNRs, respectively, but the increases were not dramatic. Sub-nanosized Au clusters significantly influenced the electronic structure and corresponding Raman characteristic of the r-GOs, whereas larger-sized AuNRs exhibited little influence. From these results, we conclude that the AuNPs with sub-nanometre size should be synthesized on the r-GOs to effectively fill the defects.

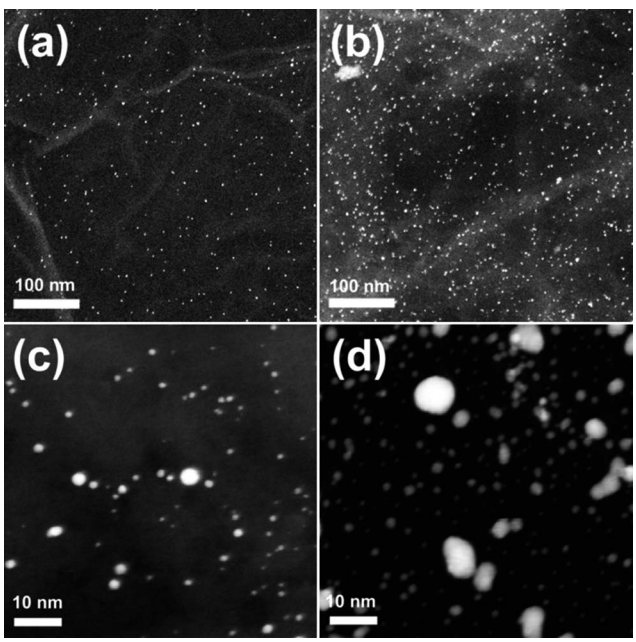

Fig. 3 The HAADF-STEM images of (a) 1-AuNP/r-GOs, (b) 4-AuNP/r-GOs, and the magnified images of (c) 1-AuNP/r-GOs, (d) 4-AuNP/r-GOs.

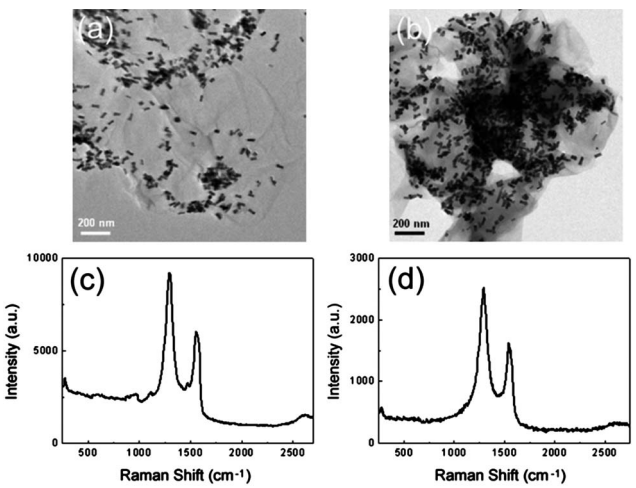

Fig. 4 TEM images of r-GOs with (a) low and (b) high loadings of AuNRs. (c), (d) Corresponding Raman spectra, respectively. Note that the negatively charged r-GOs are coated with positively charged AuNRs *via* electrostatic interactions.

The formation mechanism of Au sub-nanoclusters on r-GOs was investigated by first-principles density-functional theory (DFT) calculations (Fig. 5). Au-divacancy defect complexes in graphene using VASP code is used.[14] We employed the projector-augmented wave (PAW) potentials with a plane-wave basis set and the Perdew-Burke-Ernzernhof (PBE) exchange–correlation functional.[15] The 6 × 6 graphene supercell with 20-Å vacuum separation was used. The 4 × 4 × 1 and 12 × 12 × 1 k-points sampling were used for total energy and density of states (DOS) calculations, respectively. We used the kinetic energy cutoff of 400 eV and Gaussian smearing of 0.1 eV. All atomic forces are fully minimized less than 0.025 eV $Å^{-1}$. The binding energy of an Au atom on divacancy defect is defined as $E_{binding} = E_{divacancy} + E_{Au} - E_{Au+divacancy}$, where E is the DFT total energy of each system.

When an Au atom is adsorbed on perfect graphene, the binding energy is only 0.19 eV, falling into the van der Waals interaction range. This value is smaller than the calculated cohesive energy (3.10 eV) of face-centered cubic Au. Thus, Au atom would easily form bigger clusters on graphene if no defect presents. However, the binding energy of Au atom for filling a carbon divacancy site is calculated to be 3.40 eV, which is larger than the Au cohesive energy. Thus, the divacancy could be a nucleation site for growth of Au sub-nanoclusters.

The rectangular C_4 divacancy pores can be decorated by oxygen and nitrogen in r-GO environment. It is also reported[14b] that the N substitution at the divacancy site would be much more likely than at the perfect carbon site. Thus, we considered representative C_2N_2, N_4, N_2O_2, O_4 and O_2C_2 pores. Among them, the C_2N_2 pore most strongly holds an Au atom with the binding energy of 4.99 eV, as shown in Fig. 5a. The other N_4, N_2O_2, O_4 and O_2C_2 pores give the Au binding energies of 3.14 eV, 0.4 eV, 0.34 eV and 1.06 eV, respectively. Therefore, the C_4, C_2N_2 and N_4 pores can serve for the nucleation of Au sub-nanocluster. It is worth of note that oxygen-containing divacancy pores cannot hold an Au atom in a thermodynamic condition, because the oxygen terminals are almost self-passivated and thus their Au binding should be very weak. However, in case of a nitrogen-containing C_2N_2 pore, we could see a strong hybridization between the p orbitals of the pore terminals and the d orbitals of Au, as shown in Fig. 5c. The Au 5d orbitals almost lost their localization character.

The second Au atom can bind to the Au-divacancy complex, as shown in Fig. 5b. The calculated binding energies of the second Au are 0.65 eV, 1.01 eV and 0.87 eV, for C_4, C_2N_2 and N_4 pores, respectively. Even if the binding energy is much smaller than the cohesive energy of 3.1 eV, it is much greater than the van der Waals interaction energy of Au on graphene, 0.19 eV. Therefore, we can conclude that the nucleation and growth of the Au sub-nanoclusters would be initiated at the defect site. The local density of states analysis in Fig. 5c represents that the second Au almost preserves the atomic character with strongly localized 5d orbitals. A small energy gap is developed at the Fermi level because of the metallic s–s bonding in the Au–Au dimers. This means that the metallic Au atoms would grow into bigger nanoclusters, as more Au arrives at the site.

To appreciate detailed features in the electronic structure of C_2N_2 and Au_2-C_2N_2 incorporated r-GOs, we calculated and presented band structure diagrams of pristine, C_2N_2, Au–C_2N_2, and Au_2–C_2N_2 r-GOs (Fig. 6). As shown in Fig. 6, C_2N_2-only incorporated r-GO shows a small band gap of 0.1 eV at the Fermi level. The band gap can contribute to reduction of the electrical conductivity, compared to pristine metallic graphene. When one Au atom is incorporated into the C_2N_2 pore, however, the band gap disappears at the Fermi level as it is shifted down. The whole r-GO becomes metallic, and r-GO's linear band is electron-doped due to electron transfer from Au to r-GO. The metallic state is preserved even after another Au is introduced on top of Au–C_2N_2; the Dirac cone is still electron-doped while one can clearly see two Au's s–s dimer states (Fig. 6). Therefore, our band structure analysis shows that the presence of electron-donating Au sub-nanoclusters could contribute positively to electrical conductivity of r-GO.

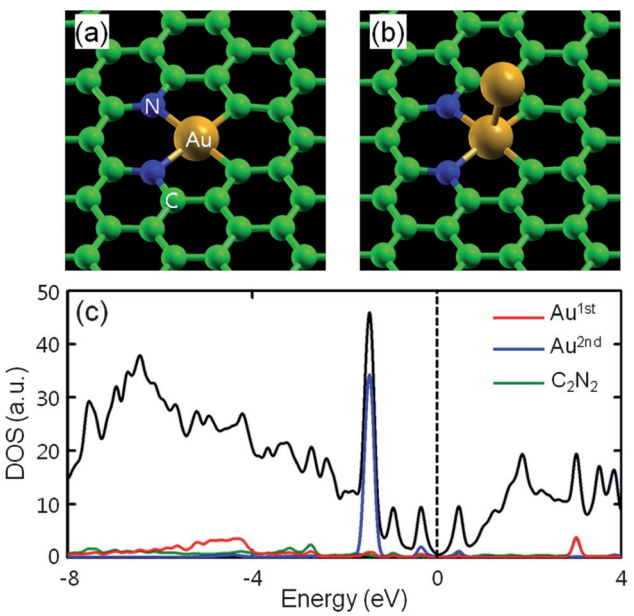

Fig. 5 Ball-and-stick view of (a) Au and (b) Au_2 sub-nanoclusters conjugated with the C_2N_2 divacancy pore of graphene. Green, blue, and light brown balls represent C, N, and Au, respectively. (c) Total and local densities of states (DOS) of the Au_2–C_2N_2 incorporated graphene in (b) near the Fermi level, set to 0 eV. The black line indicates the total DOS, and the red, blue, and green lines indicate the local DOSs of the first Au adatom, the second Au adatom, and the C_2N_2 pore, respectively.

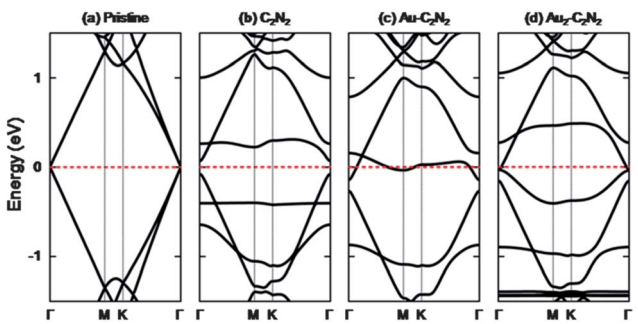

Fig. 6 DFT band structures of (a) pristine (6 × 6) graphene, and (b) C_2N_2, (c) Au–C_2N_2 and (d) Au_2–C_2N_2 incorporated (6 × 6) graphenes near the Fermi energy, marked by the red dotted line.

Based on the above information, we believe that the initial Au atom nucleates in the defective sites of r-GO, particularly divacant nitrogen sites by forming strong covalent bonds between them. The Au-divacancy defects cannot be inactive for the Raman D band excitation. Thus, the reduction of the Raman D peak upon Au growth should be explained by filling of the nitrogen defects with Au atoms, leading to the restoration of flat geometry of graphene. Because significant amount of the nitrogen defects are in the r-GOs (21.03%),[16] the filling effect of the defects with Au atoms would be prominent (Fig. 7).

Conclusions

In summary, we have demonstrated a novel approach for filling the defects on the r-GOs using sub-nanosized Au clusters. This approach resulted in a dramatic decrease in the I_D/I_G ratio with a concurrent increase in the conductivity of the r-GOs. As the growth cycle was repeated, the defects were gradually filled by the increasing number of sub-nano Au clusters. This filling effect led to a dramatic change in the electric properties of the resulting r-GOs. Furthermore, such property changes can be reversed by elimination of the synthesized AuNPs from the surface of the r-GOs. It is verified that Au atom can fill various divacancy pores, particularly the C_2N_2 pore of graphene, which could be a nucleation center for further growth of Au sub-nanoclusters. Our approach could be useful for enhancing the conductivity of chemically synthesized r-GOs, which generally exhibit diminished conductivities compared to those prepared by CVD. This research could also be useful in the development of novel nanocomposites, such as a nanofiller with a high conductivity. In addition, these results could provide an opportunity for tailoring the electronic structure of r-GOs by the simple growth of metal NPs. We envision that a variety of novel r-GOs with interesting properties could be prepared by changing the type of inorganic NPs used; such investigations will be the subject of future investigations.

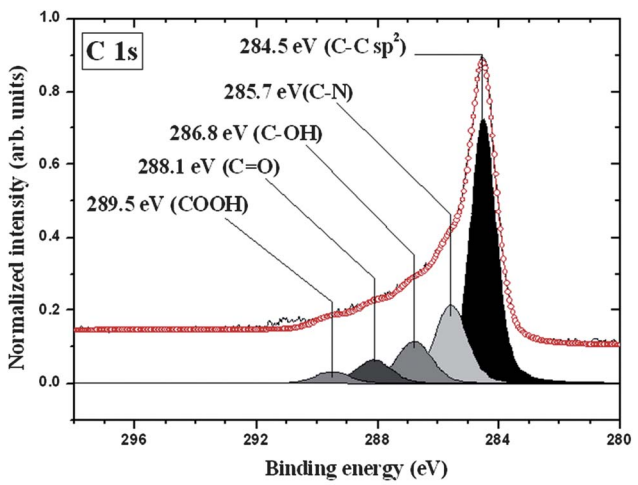

C-C sp^2	C-N	C-OH	C=O	COOH	Total
284.5 eV	285.7 eV	286.8 eV	288.1 eV	289.5 eV	
57.94	21.03	11.95	6.45	2.63	100

Fig. 7 The C1s XPS spectra of r-GOs prepared by oxidation-reduction process. It clearly indicates a considerable degree of oxidation with four components that correspond to carbon atoms in different functional groups: the non oxygenated ring C, the C in C–O bonds, the carbonyl C, and the carboxylate carbon (O–C=O). The additional peak at 285.7 eV corresponds to C bound to nitrogen. Among the defects, the content of nitrogen defects is much higher than that of the others.

Experimental

Materials

The H_2SO_4, HNO_3, gold chloride trihydrate ($HAuCl_4 \cdot 3H_2O$, 99.9%) and $NaBH_4$ were purchased from Sigma-Aldrich and used as received. Graphite powder was purchased from GK (product MGR 25 998 K). Deionized (DI) water with a resistance of 18.2 MΩ cm was obtained from a Millipore Simplicity 185 system.

Preparation of graphite oxide

The graphite oxides were prepared according to the previously reported method. Graphite powder (1 g) was placed into a cold concentrated H_2SO_4 solution (23 mL) with stirring. Solid $KMnO_4$ (3 g) was gradually added with stirring and cooling to prevent a rapid increase in the temperature of the mixture (should be less than 20 °C). After removal from the ice bath, the reaction mixture was stirred for 30 min at room temperature. DI water (23 mL) was slowly added to the reaction vessel while the temperature was maintained below 95 °C. After 15 min, the reaction was terminated by the addition of a large amount of DI water (150 mL), followed by the addition of 10 mL of H_2O_2 (30%) solution. After reacting overnight, the resulting solution was subjected to dialysis until the pH of the solution reached 7 to ensure complete removal of the metal ions and acids. After centrifugation and freeze drying, the resulting GO powder was obtained.

Preparation of graphene nanosheets (GNS)

The graphene nanosheets (GNSs) were prepared by hydrazine reduction of the prepared GO powders. Typically, 30 mg of GO powder was placed in 30 mL of DI water and ultrasonicated for 1 h. To reduce the GO solution, 0.2 mL of hydrazine was added to the solution at 100 °C under a water-cooled condenser and under a N_2 gas purge. After overnight reaction, the resulting solution was filtered or centrifuged to remove the unreacted PSS.

Preparation of Au/r-GOs

A 1.5 mL aqueous solution containing a $HAuCl_4$ (6.7 mg/1.5 mL) was prepared and mixed with 0.1 mL of an aqueous suspension of r-GOs (0.05 wt%). The dispersion was vigorously agitated on a shaking apparatus for 4 h to allow the Au ions to adsorb to the r-GOs. The Au ions adsorbed on the r-GOs were reduced by addition of $NaBH_4$ (1 mL). After 30 min, the dispersion was centrifuged at 15 000 g for 3 min, the supernatant was removed, and 1.4 mL of water was added. This rinsing step was repeated three times. The above procedure was performed a total of one, two, three, and four times to prepare the 1-, 2-, 3-, and 4-Au/r-GOs, respectively.

Characterization

FE-TEM and HAADF-STEM analyses were carried out using a JEOL (JEM-2200 FS) microscope operated at 200 kV. Raman analyses were performed using a scanning confocal Raman microscope (Nanofinder 30, Tokyo Instruments). XPS studies were carried out on an Axis NOVA (Kratos analytical) spectrometer, using an aluminium anode (Al KR, 1486.6 eV) operated at 600 W. Conductivity measurements of the Au/r-GOs (4-, 3-, 2-, 1-, and 0-Au/r-GOs) films prepared by vacuum filtration were carried out on a MST 4000A Test Unit using a four-point-probe head with a pin-distance of about 1 mm.

Acknowledgements

This work was supported by the Korea Institute of Science and Technology (KIST) institutional program, the Fundamental R & D program from Jeollabuk-do (101932), WCU program (R31-2008-000-10071-0), Basic Science Research program (2010-0006922), and the Korea Basic Science Institute (KBSI).

Notes and references

1 (*a*) K. S. Novoselov, A. K. Geim, S. V. Morozov, D. Jiang, Y. Zhang, S. V. Dubonos, I. V. Grigorieva and A. A. Firsov, *Science*, 2004, **306**, 666; (*b*) S. Stankovich, D. A. Dikin, G. H. B. Dommett, K. M. Kohlhaas, E. J. Zimney, E. A. Stach, R. D. Piner, S. T. Nguyen and R. S. Ruoff, *Nature*, 2006, **442**, 282; (*c*) M. D. Stoller, S. Park, Y. Zhu, J. An and R. S. Ruoff, *Nano Lett.*, 2008, **8**, 3498.
2 (*a*) W. S. Hummers and R. E. Offeman, *J. Am. Chem. Soc.*, 1958, **80**, 1339; (*b*) S. Park and R. S. Ruoff, *Nat. Nanotechnol.*, 2009, **4**, 217.
3 (*a*) S. Grimme, C. Muck-Lichtenfeld and J. Antony, *J. Phys. Chem. C*, 2007, **111**, 11199; (*b*) Z. B. Liu, Y. F. Xu, X. Y. Zhang, X. L. Zhang, Y. S. Chen and J. G. Tian, *J. Phys. Chem. B*, 2009, **113**, 9681; (*c*) J. Geng and H. Jung, *J. Phys. Chem. C*, 2010, **114**, 8277; (*d*) H. Bai, C. Li and G. Shi, *Adv. Mater.*, 2011, **23**, 1089.
4 H. Y. Koo, H. J. Lee, H. A. Go, Y. B. Lee, T. S. Bae, J. K. Kim and W. S. Choi, *Chem.–Eur. J.*, 2011, **17**, 1214.
5 (*a*) R. Muszynski, B. Seger and P. V. Kamat, *J. Phys. Chem. C*, 2008, **112**, 5263; (*b*) G. Goncalves, P. A. A. P. Marques, C. M. Granadeiro, H. I. S. Nogueira, M. K. Singh and J. Grácio, *Chem. Mater.*, 2009, **21**, 4796; (*c*) J. Liu, S. Fu, B. Yuan, Y. Li and Z. Deng, *J. Am. Chem. Soc.*, 2010, **132**, 7279; (*d*) G. Lu, S. Mao, S. Park, R. S. Ruoff and J. Chen, *Nano Res.*, 2009, **2**, 192.
6 M. A. Pimenta, G. Dresselhaus, M. S. Dresselhaus and L. G. Cancado, *Phys. Chem. Chem. Phys.*, 2007, **9**, 1276.
7 (*a*) H. M. A. Hassan, V. Abdelsayed, A. E. R. S. Khder, K. M. AbouZeid, J. Terner, M. S. El-Shall, S. I. Al-Resayes and A. A. El-Azhary, *J. Mater. Chem.*, 2009, **19**, 3832; (*b*) B. S. Kong, J. X. Geng and H. T. Jung, *Chem. Commun.*, 2009, 2174; (*c*) W. Hong, H. Bai, Y. Xu, Z. Yao, Z. Gu and G. Shi, *J. Phys. Chem. C*, 2010, **114**, 1822; (*d*) Y. Fang, S. Guo, C. Zhu, Y. Zhai and E. Wang, *Langmuir*, 2010, **26**, 11277.
8 S. Stankovich, R. D. Piner, X. Chen, N. Wu, S. T. Nguyen and R. S. Ruoff, *J. Mater. Chem.*, 2006, **16**, 155.
9 (*a*) R. Voggu, B. Das, C. S. Rout and C. N. R. Rao, *J. Phys.: Condens. Matter*, 2008, **20**, 472204; (*b*) R. A. Jishi and M. S. Dresselhaus, *Phys. Rev. B: Condens. Matter*, 1992, **45**, 6914; (*c*) Q. Su, S. Pang, V. Alijani, C. Li, X. Feng and K. Müllen, *Adv. Mater.*, 2009, **21**, 3191.
10 K. S. Subrahmanyam, A. K. Manna, S. K. Pati and C. N. R. Rao, *Chem. Phys. Lett.*, 2010, **497**, 70.
11 (*a*) R. Anton and I. Schneidereit, *Phys. Rev. B: Condens. Matter*, 1998, **58**, 13874; (*b*) J. A. Rodríguez-Manzo, O. Cretu and F. Banhart, *ACS Nano*, 2010, **4**, 3422.
12 E. Yoo, T. Okata, T. Akita, M. Kohyama, J. Nakamura and I. Honma, *Nano Lett.*, 2009, **9**, 225.
13 Y. Okamoto, *Chem. Phys. Lett.*, 2006, **420**, 382.
14 (*a*) D. H. Lee, W. J. Lee, S. O. Kim and Y. H. Kim, *Phys. Rev. Lett.*, 2011, **106**, 175502; (*b*) W. I. Choi, S. H. Jhi, K. Kim and Y. H. Kim, *Phys. Rev. B: Condens. Matter Mater. Phys.*, 2010, **81**, 085441; (*c*) G. Kresse and D. Joubert, *Phys. Rev. B: Condens. Matter Mater. Phys.*, 1999, **59**, 1758.
15 (*a*) P. E. Blöchl, *Phys. Rev. B: Condens. Matter*, 1994, **50**, 17953; (*b*) J. P. Perdew, K. Burke and M. Ernzerhof, *Phys. Rev. Lett.*, 1996, **77**, 3865.
16 (*a*) D. Briggs and G. Beamson, *The Scienta ESCA 300 Database*, New York, John Wiley and Sons, 1992; (*b*) R. J. Waltman, J. Pacansky and C. W. Jr. Bates, *Chem. Mater.*, 1993, **5**, 1799.